

<sup>1</sup>Angel ZUMBILEV, <sup>2</sup>Hristian PANAYOTOV, <sup>3</sup>Iliya ZUMBILEV

## METHODOLOGY FOR ROENTGENOGRAPHIC DETERMINATION OF RESIDUAL STRESSES IN SURFACE LAYERS

<sup>1,3</sup>TECHNICAL UNIVERSITY SOFIA – PLOVDIV BRANCH, DEPARTMENT OF MATERIAL SCIENCE AND TECHNOLOGY

<sup>2</sup>TECHNICAL UNIVERSITY SOFIA – PLOVDIV BRANCH, DEPARTMENT OF AVIATION ENGINEERING, BULGARIA

**ABSTRACT:** The aim of the present work is to examine the influence of nitriding and carbonitriding in low-temperature plasma on formation of residual macro-stresses in the treated layers. Two different modes of ion-nitriding and carbonitriding are viewed. The resulting layers have specific thickness and surface micro-hardness and different values for the residual stresses. Algorithm and methodology for calculation of the residual stresses in the diffusive zone of layers using regression analysis in MATLAB is given. The results show that ion-carbonitrided layers have greater residual macro-stresses than ion-nitrided ones.

**KEYWORDS:** ion-nitriding and carbonitriding, residual compressive stresses, methodology

### ❖ INTRODUCTION

The requirements for high quality in machine parts and assemblies are directly linked to their reliability and durability that in their turn depend on the internal stresses of parts.

Internal stresses practically appear in all parts. Defined by their different action radius in the structure of the body, internal stresses are mainly three types that differ from each other.

The first type internal stresses, also called macro-internal stresses, can be found in the volume of a few grains depending on their value and direction. The associated with this type of stresses internal forces act both on each area of the cross-section and on the whole body in equilibrium. The internal momentums related to them also disappear along each of the axes. In case of action on the force and momentum equilibrium of bodies with first type internal stresses macroscopic changes in the body size occur.

The second type internal stresses, also known as micro-stresses, are approximately homogeneous in the volume of a grain. They are formed between differently oriented in space crystallites as well as between phases with different hardness quality. The equilibrium between the internal forces and the internal stresses propagates over majority of grains. After removing the load, correspondingly, in the harder volumes and in crystals, unfavorably oriented with respect to the direction of the load, strain stresses occur, opposite to which compressive stresses act on the side of the softer volumes and crystals with more favorable orientation with respect to the direction of the load.

The third type internal stresses (non-homogeneous micro-stresses) are non-homogeneously distributed. The equilibrium between the internal forces and momentums propagates over parts of a grain. Actions on the force and momentum equilibrium do not cause microscopic changes in the size of a given body.

Since the values of the internal stresses are often below the limit of flow of the corresponding material, their measuring is highly demanding to the measuring equipment. There are plenty of methods for defining the internal stresses and they can be divided into the following two groups: destructive methods - the methods of disassembling, of hanging down (the slack method), of drilling, boring and trimming; non-destructive methods - the Roentgen method, the magnetic method, the ultrasound method and the neutron rays method [7].

The Roentgenographic method allows registering submicroscopic changes in the distances between the atoms corresponding to the measured planes in the crystal lattice of the grains for a mono-crystal material. It is a completely non-destructive method. Because of the limited depth of penetration of the X-rays, which, for steel is  $l \leq 20\mu\text{m}$ , only the tense state of the closest to the surface layer is registered.

The calculation principle used here allows determining of only two-axial internal stresses, parallel to the surface.

The distance between the atoms in the crystal lattice is normally about several nanometers. The wave length  $\lambda$  of the X-rays is also several dozens of nanometers, i.e., these quantities are of the same order. Therefore the Roentgen rays are considered to be among the most reliable for investigating the crystal structure [8,9,10,12].

One of the basic methods of increasing the wear resistance of details is the purposeful improvement of their surface layer properties by means of mechanical, thermal, chemical-thermal and other types of hardening treatment [1,2,3,4,11,13]. A task of present interest with a view to increasing the effectiveness of the technologies, developed on the purpose, is the investigation of internal stresses in the materials, resulting from the corresponding treatment [5, 6].

The aim of the present work is to develop a methodology for defining the residual stresses formed on the surface of 25CrMnSiNiMo steel after ion nitriding and carbonitriding.

#### ❖ MATERIALS UNDER INVESTIGATION AND MODES OF THERMAL TREATMENT

25CrMnSiNiMo steel is the material under investigation; its chemical composition is checked by the equipment for automatic analysis "Spectrotest" and given in Table 1.

Table 1. CHEMICAL COMPOSITION OF THE INVESTIGATED STEEL

Material	Chemical elements, weight percentage							
	C	Cr	Mo	Ni	P	Si	Mn	S
25CrMnSiNiMo	0,24	0,87	0,12	1,36	0,002	1,45	1,28	0,002

The requirement for a preliminary thermal treatment is imposed mainly by the following consideration: for achieving the desired mechanical parameters and structure, enabling a favorable process of nitrogen diffusion in depth. The investigated steel is thermally treated in a chamber furnace under modes, given in Table 2.

Table 2. Modes of preliminary thermal treatment

Material	T <sub>hard.</sub> [°C]	Cooling medium	T <sub>temp.</sub> [°C]	Cooling medium
25CrMnSiNiMo	900	Oil	600	Air

Treated thermally this way, the samples are then subjected to ion carbonitriding in the installation "Ion-20", following the modes given in Table 3. Ammonia (NH<sub>3</sub>) is used as saturating gas during the process of nitriding, while during the process of carbonitriding the combination of ammonia and corgon (82 % Ar and 18% CO<sub>2</sub>) in different percentage ratio is used. The temperature of treatment for both processes - nitriding and carbonitriding - is 550°C.

Table 3. Modes of ion nitriding and carbonitriding

Mode №	Sample №	Material	$\tau$ [h]	P <sub>1</sub> ammonia [Pa]	P <sub>2</sub> corgon [Pa]	P [Pa]	U [V]
1	888	25CrMnSiNiMo	2	400	-	400	530
2	90	25CrMnSiNiMo	2	200	200	400	415

#### ❖ ROENTGENOGRAPHIC DETERMINATION OF INTERNAL STRESSES

The investigation of the internal stresses in the nitrided and carbonitrided samples is performed by means of a Roentgen diffraction-meter SET-X ENSAM, following the „sin<sup>2</sup> $\Psi$ ” method.

The direction of measuring is characterized by the angle  $\Psi$ : 0°, 14.96°, 21.42°, 26.57°, 31.09°, 35.26°, 37.23°, -10,52°, -18.43°, -24.09°, -28.88°, -33.21°, -37.27° and the angles  $\varphi$ :  $\varphi=0$  and  $\varphi=90$ .

A powdered sample is used for standardizing the Roentgen diffraction-meter. Since the powdered sample is free of residual stresses, it allows checking and easily adjusting the device. In this particular case chromium Roentgen radiation Cr - K $\alpha$  with a wave-length of  $\lambda=2.29\text{\AA}$  was used. Information about the formed stresses is given at a distance of 2 $\mu\text{m}$  in the plane  $\alpha$  - Fe {2 1 1} under the combined zone.

For calculating the residual stresses in the layers the following elasticity constants are chosen: Poisson's ratio  $\mu = 0,29$ , elasticity modulus  $E = 210$  Gpa. The master diffraction angle  $2\theta = 156^{\circ}30'$ , and  $\theta = 78^{\circ}15'$ . The miscount at defining stresses depends on the relative mistake  $\Delta\theta/\theta$  at defining the angle  $\theta$ . It is within 2-3%. By means of the Roentgen diffraction-meter the diffraction angles in the carbonitrided and nitrided layers (Table 4, Table 5) are measured at different angles of rotation of the sample. The obtained data are introduced into the MATLAB programme, by means of which graphs are built and the values of angle  $2\theta$  for sin<sup>2</sup> $\Psi$  are defined at  $\Psi=90^{\circ}$  - Figure 2, Figure 3.

❖ RESULTS AND ANALYSIS

In order to calculate the residual stresses in nitrided and carbonitrided layers an algorithm and a methodology are developed (Fig. 1). The experimental results, shown in Table 4 and Table 5, serve as an input. The calculation of residual stresses requires determination of previously unknown value of  $2\theta$  at  $\Psi=90^\circ$ . In the present work an attempt is made to estimate this value using regression analysis. Based on given experimental data a linear least-squares polynomial approximation is used to derive the equation  $y=y_0+kx$ .

Depending on the input experimental data and its variance two cases are possible: the approximation equation is an adequate representation of the experimental data; or the approximation equation is not an adequate representation of the experimental data. This check is done using the F-Fisher criterion.

If the result from the check is positive then the estimate values for  $2\theta$  at  $\Psi=90^\circ$  are determined by means of extrapolation. Thus the residual stresses in the treated layer can be calculated. If the result from the F-Fisher check is negative then some additional experiments should be conducted.

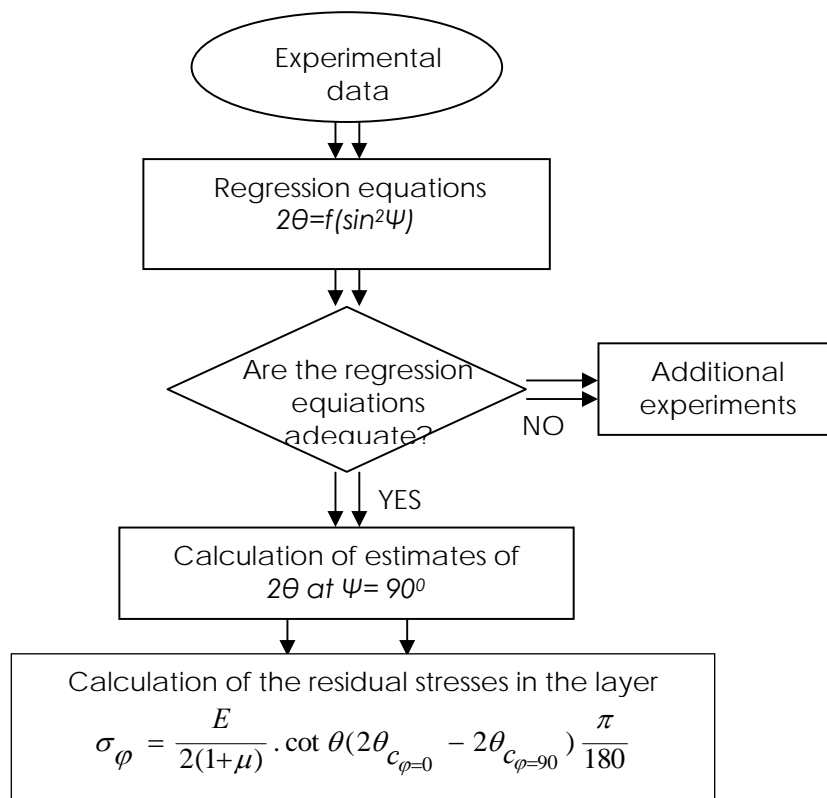


Fig. 1. ALGORITHM FOR DETERMINATION OF RESIDUAL STRESSES

In this case, two objects of study are considered, namely nitrided sample 90 and carbonitrided sample 888.

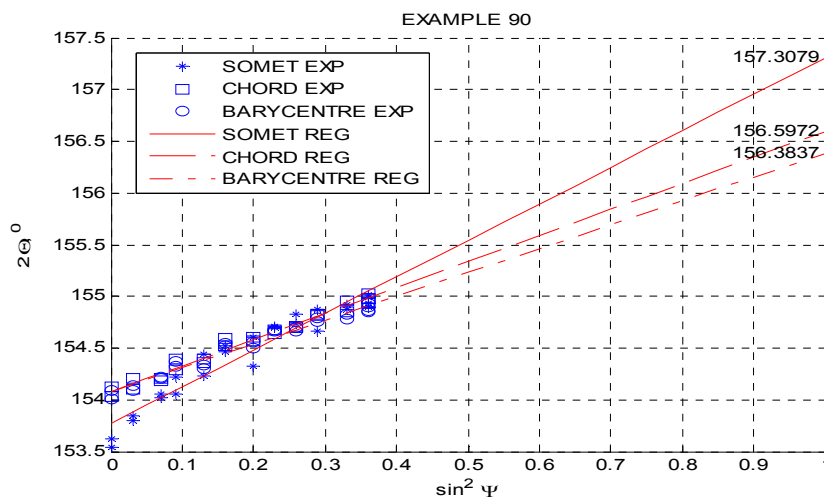


Fig. 2. Data approximation for model 90

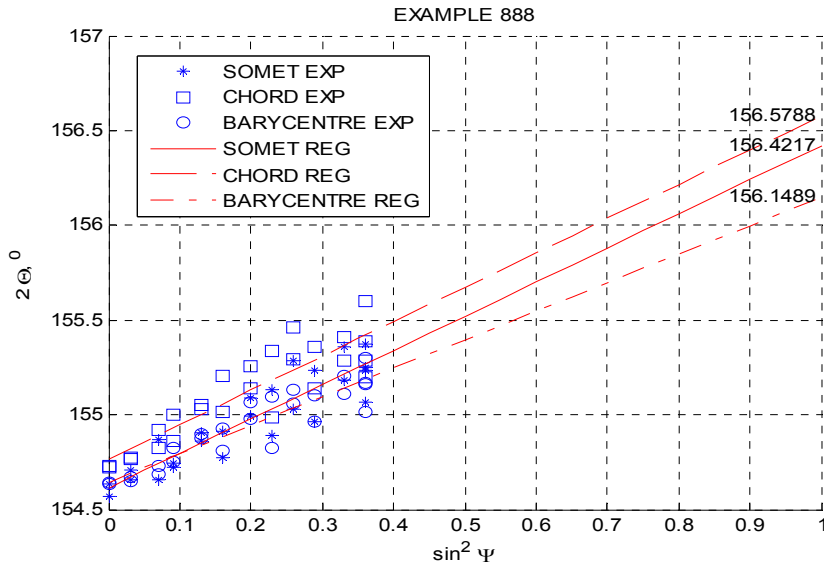


Fig. 3. Data approximation for model 888

For each sample three polynomial regressions are created. They represent a linear approximation of the functions  $2\theta^s$ ,  $2\theta^c$ ,  $2\theta^b$  of the angle  $\psi$ . An important step in regression analysis is the adequacy check that is done by determination of the variance of the Y index to its mean value  $\bar{Y}$ ,

$$S_{\bar{Y}}^2 = \frac{1}{n-1} \sum_{j=1}^n (y_j - \bar{Y})^2 \tag{1}$$

Table 4. Diffraction angles measured after rotation of the carbonitrided sample 90 at angles  $\psi$  and  $\Phi$

$\varphi$	$\psi$	$\sin^2 \psi$	2 $\theta_s$	2 $\theta_c$	2 $\theta_b$
0	0	0	153,617	154,12	154,091
0	14,96	0,07	154,015	154,205	154,214
0	21,42	0,13	154,441	154,355	154,341
0	26,57	0,2	154,605	154,567	154,501
0	31,09	0,26	154,824	154,708	154,661
0	35,26	0,33	154,92	154,852	154,779
0	37,23	0,36	155,02	154,974	154,899
0	-10,52	0,03	153,847	154,205	154,14
0	-18,43	0,09	154,058	154,396	154,375
0	-24,09	0,16	154,464	154,528	154,523
0	-28,88	0,23	154,71	154,643	154,675
0	-33,21	0,29	154,669	154,824	154,757
0	-37,27	0,36	154,93	154,979	154,868
-90	0	0	153,546	154,033	154,014
-90	14,96	0,07	154,061	154,19	154,204
-90	21,42	0,13	154,232	154,394	154,303
-90	26,57	0,2	154,32	154,601	154,557
-90	31,09	0,26	154,73	154,702	154,698
-90	35,26	0,33	154,877	154,961	154,823
-90	37,23	0,36	154,99	154,937	154,848
-90	-10,52	0,03	153,803	154,098	154,092
-90	-18,34	0,09	154,219	154,292	154,33
-90	-24,09	0,16	154,526	154,589	154,549
-90	-28,88	0,23	154,695	154,679	154,665
-90	-33,21	0,29	154,874	154,818	154,793
-90	-37,27	0,36	154,894	155,025	154,927

Table 5. Diffraction angles measured after rotation of the nitrided sample 888 at angles  $\psi$  and  $\Phi$

$\varphi$	$\psi$	$\sin^2 \psi$	2 $\theta_s$	2 $\theta_c$	2 $\theta_b$
0	0	0	154.635	154.726	154.646
0	14.96	0.07	154.655	154.923	154.73
0	21.42	0.13	154.86	155.049	154.901
0	26.57	0.2	155.091	155.259	155.068
0	31.09	0.26	155.03	155.295	155.131
0	35.26	0.33	155.36	155.409	155.207
0	37.23	0.36	155.372	155.602	155.299
0	-10.52	0.03	154.705	154.771	154.672
0	-18.43	0.09	154.747	154.865	154.752
0	-24.09	0.16	154.775	155.017	154.809
0	-28.88	0.23	154.888	154.988	154.828
0	-33.21	0.29	154.962	155.141	154.963
0	-37.27	0.36	155.067	155.197	155.017
-90	0	0	154.57	154.728	154.638
-90	-10.52	0.03	154.655	154.764	154.65
-90	-18.43	0.09	154.724	155.001	154.822
-90	-24.09	0.16	154.915	155.202	154.931
-90	-28.88	0.23	155.13	155.338	155.099
-90	-33.21	0.29	155.233	155.356	155.1
-90	-37.27	0.36	155.252	155.285	155.171
-90	14.96	0.07	154.871	154.823	154.684
-90	21.42	0.13	154.905	155.031	154.875
-90	26.57	0.2	154.995	155.143	154.981
-90	31.09	0.26	155.285	155.458	155.057
-90	35.26	0.33	155.18	155.284	155.108
-90	37.23	0.36	155.237	155.39	155.161

Then the residual variance is calculated:

$$S_{OCT}^2 = \frac{1}{n-m'} \sum_{j=1}^n (y_j - \hat{y}_j)^2 \tag{2}$$

where:  $n$  - number of the experimental points;  $m'$  - number of coefficients;  $y_j$  - the  $j$ -value of  $Y$  from the experiment;  $\hat{y}_j$  - the  $j$ -predicted value of  $Y$ .

Using these two variances the value of the criterion is calculated:

$$F_0 = \frac{S_{\bar{y}}^2}{S_{OCT}^2} \quad (3)$$

The critical value of the criterion  $F_{\alpha; k_1; k_2}$  at degrees of freedom  $k_1 = n - 1$ ,  $k_2 = n - m'$  and 95% confidence interval is determined. If  $F_0 \geq F_{\alpha; k_1; k_2}$ , then the regression equation can be used for prediction, optimization, etc. In the present research according to table 4 and table 5  $F_{\alpha; k_1; k_2} = F_{0,05; 25; 24} = 1,73$ .

In table 6 and table 7 are given respectively: coefficients of the regression equations  $y_0$  and  $k$ ; standard deviation of the experimental data; calculated  $S_{\bar{y}}^2$ ,  $S_{OCT}^2$  and  $F_0$  for each regression equation. The adequacy check shows that the regressions are statistically accurate approximation and they can be used to predict the value of  $2\theta$  at  $\psi = 90^\circ$  ( $\sin^2\psi = 1$ ). These values are shown on figures 2 and 3. Applying the described methodology on the test samples the compressive stresses in the nitrided and carbonitrided layer are calculated. Three methods of calculation are used: maximum intensity method -  $\sigma_\varphi^s$ ; chord method -  $\sigma_\varphi^c$ ; centre-of-gravity method -  $\sigma_\varphi^b$ .

Table 6. Results from the regression analysis of the carbonitrided sample

	$y_0$	$k$	$\sigma$	$S_{\bar{y}}^2$	$S_{OCT}^2$	$F_0$	$F_0 > F_{0,05; 25; 24}$
SOMET	153.77	3.5328	0.1253	0.1982	0.0146	13.58	ΔA
CHORD	154.07	2.5192	0.0494	0.0958	0.0023	42.35	ΔA
BARYCENTRE	154.07	2.3045	0.0537	0.0809	0.0027	30.24	ΔA

Table 7. Results from the regression analysis of the nitrided sample

	$y_0$	$k$	$\sigma$	$S_{\bar{y}}^2$	$S_{OCT}^2$	$F_0$	$F_0 > F_{0,05; 25; 24}$
SOMET	154.61	1.8048	0.1067	0.0582	0.0106	5.50	ΔA
CHORD	154.76	1.8115	0.1194	0.0611	0.0132	4.61	ΔA
BARYCENTRE	154.64	1.5048	0.0815	0.0393	0.0062	6.38	ΔA

Table 8. Results from the obtained residual stresses

Material (Sample)	$\tau$ [h]	$P_1$ ammonia [Pa]	$P_2$ corgon [Pa]	HV <sub>0,1</sub>	$\delta_{06}$ [ $\mu\text{m}$ ]	$\delta_{c,3}$ [ $\mu\text{m}$ ]	$\sigma_\varphi^s$ [MPa]	$\sigma_\varphi^c$ [MPa]	$\sigma_\varphi^b$ [MPa]
25CrMnSiNiMo (90)	2	200	200	890	150	4.5	-881	-744	-680
25CrMnSiNiMo (88)	2	400	-	860	170	6.1	-535	-533	-444

After ion nitriding of sample 888 (Table 8) made of 25CrMnSiNiMo steel at:  $t_{\text{nit.}} = 550^\circ\text{C}$ ,  $P_{\text{NH}_3} = 400\text{Pa}$ ,  $\tau = 2\text{h}$ , a nitrided layer with total thickness of  $\delta_{\text{tot}} = 170\mu\text{m}$ , combined zone thickness of  $\delta_{\text{cz}} = 6.1\mu\text{m}$  and maximum micro-hardness of 860HV0.1 is obtained. In the diffusion zone of the nitrided layer formed this way residual compressive stresses of different value appear, with highest obtained value  $\sigma_\varphi^s = -535\text{MPa}$ .

By introducing of corgon (82 % Ar and 18% CO<sub>2</sub>) into the vacuum chamber at the following mode of treatment:  $t = 550^\circ\text{C}$ ,  $P_{\text{NH}_3} = 200\text{Pa}$ ,  $P_{\text{corgon}} = 200\text{Pa}$ ,  $\tau = 2\text{h}$ , a carbonitrided layer with total thickness of  $\delta_{\text{tot}} = 150\mu\text{m}$ , combined zone thickness of  $\delta_{\text{cz}} = 4,5\mu\text{m}$  and maximum micro-hardness of 890HV0.1 is obtained.

In the carbonitrided layer formed this way residual compressive stresses of higher value  $\sigma_\varphi^s = -881\text{MPa}$  than in the nitrided layer ( $\sigma_\varphi^s = -535\text{MPa}$ ) appear.

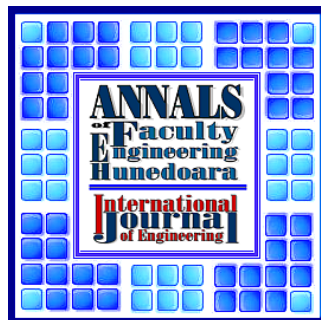
In the process of carbonitriding of 25CrMnSiNiMo steel a diffusion zone is formed, having a bigger specific volume than the diffusion zone of the nitrided layer. This can be explained by the availability of carbon dioxide in the vacuum chamber, which is half of the ammonia contents. As a result of the processes of dissociation and ionization carbon atoms are formed, having a bigger ion radius [ $r_{\text{ion}} = 16(4+1)\text{pm}$ ] than the nitrogen atoms [ $r_{\text{ion}} = 13(5+1)\text{pm}$ ]. Both elements diffuse into the vacant places between the knots of the lattice, and the change in the period of the volume-centered cubic lattice of the diffusion zone in the carbonitrided layer is bigger than it is in the nitrided layer. This leads to greater stresses in the carbonitrided layer.

## ❖ CONCLUSION

- It has been established that after ion nitriding the residual compressive stresses formed in the diffusion zone of carbonitrided samples are of higher value than they are in nitrided samples.
- A methodology for determination of residual stresses formed in nitrided and carbo-nitrided layers in the plasma of a smoldering discharge has been suggested.

## ❖ REFERENCES

- [1.] T.Lampe: Plasmawärmebehandlung von Eisenwerkstoffen in stickstoff-und kohlenstoffhaltigen Gasgemischen, VDI-Verlag GmbH, Düsseldorf, 1985, p.288.
- [2.] R.Chatterjee-Fisher, F.W.Eysell, R.Hoffman, D.Liedtke, H.Mallener, W.Rembges, A.Schreiner, G.Welker: Nitrieren und Nitrocarburieren, Expert Verlag, 1994, p.254
- [3.] V. Z.Toshkov: Nitriding in low-temperature plasma, King, Sofia, 2004, p. 242.
- [4.] R.F. Hoffman: Effects of Nitrogen in Metal Surfaces, Proceeding of an International Conference on Ion Nitriding, Cleveland, Ohio, USA 15-17, September 1989, pp. 23-30.
- [5.] Contract Heat Treatment Association: Nitriding and Nitrocarburising, Secretariat: c/o WHTC, Aston University, Aston Triangle, Birmingham B4 7ET, UK, 1996, pp. 1-2.
- [6.] V.Z. Toshkov: Theoretical and practical aspects of nitriding of iron and iron-carbon alloys in low-temperature plasma, (Ph.D. thesis, Sofia Technical University), 1997.
- [7.] M.E. Hilley: Residual Stress Measurement by X-ray Diffraction, SAE J784a, Society of Automotive Engineers, Warrendale, PA, 1971, pp. 21-24.
- [8.] Standard Method for Verifying the Alignment of X-ray Diffraction Instrumentation for Residual Stress Measurement, E 915, Annual Book of ASTM Standards, Vol 03.01, ASTM, Philadelphia, 1984, pp. 809-812.
- [9.] P.S. Prevey: A comparison of X-ray diffraction residual stress measurement methods of machined surfaces /advances in X-ray analyses, 1976, V 19, pp. 709-724.
- [10.] A. da Silva Rocha, T. Strohecker, V. Tomala, T. Hirsch: Microstructure and residual stresses of a plasma-nitrided M2 tool steel, Surface and Coatings Technology, 115, 1999, pp. 24-31.
- [11.] T. Bell, Y Sun, A. Suhadi: Environmental and technical aspects of plasma nitrocarburising, Vacuum, 59, 2000, pp. 14-23.
- [12.] C.Kanchanomai, W.Limtrakarn: Effect of Residual Stress on Fatigue Failure of Carbonitrided Low-Carbon Steel. Materials Engineering and Performance, Volume 17, Issue 6, 2008, pp.879-887.
- [13.] V. Campagna, R. Bowers, D.O. Northwood X. Sun, P. Bauerle: The Nitrocarburizing of Plain Carbon Steel Automotive Components, Proceedings of the 24th ASM Heat Treating Society Conference, September 17-19, COBO Center, Detroit, Michigan, USA, 2007, pp. 239-244.
- [14.] Matlab 2010 Statistic Toolbox™, MathWorks® , 2010



**ANNALS OF FACULTY ENGINEERING HUNEDOARA  
– INTERNATIONAL JOURNAL OF ENGINEERING**

copyright © University Politehnica Timisoara,

Faculty of Engineering Hunedoara,

5, Revolutiei, 331128, Hunedoara,

ROMANIA

<http://annals.fih.upt.ro>